ACCOUNTS of chemical research

Article

pubs.acs.org/accounts

Interfacial Donor–Acceptor Engineering of Nanofiber Materials To Achieve Photoconductivity and Applications

Ling Zang*

Nano Institute of Utah, Department of Materials Science and Engineering, Department of Chemistry, University of Utah, Salt Lake City, Utah 84112, United States

CONSPECTUS: Self-assembly of π-conjugate molecules often leads to formation of well-defined nanofibril structures dominated by the columnar $\pi-\pi$ stacking between the molecular planes. These nanofibril materials have drawn increasing interest in the research frontiers of nanomaterials and nanotechnology, as the nanofibers demonstrate one-dimensionally enhanced exciton and charge diffusion along the long axis, and present great potential for varying optoelectronic applications, such as sensors, optics, photovoltaics, and photocatalysis. However, poor electrical conductivity remains a technical drawback for these nanomaterials. To address this problem, we have developed a series of nanofiber structures modified with different donor–acceptor (D–A) interfaces that are tunable for maximizing the photoinduced charge separation, thus leading to increase in the electrical conductivity. The D–A interface can be constructed with covalent linker or noncovalent interaction (e.g., hydrophobic interdigitation between alkyl chains). The noncovalent method is generally more flexible for molecular design and solution processing, making it more adaptable to be applied to other fibril nanomaterials such as carbon nanotubes. In this Account, we will discuss our recent discoveries in these research fields, aiming to provide deep insight into the enabling photoconductivity of nanofibril materials, and the dependence on interface structure.

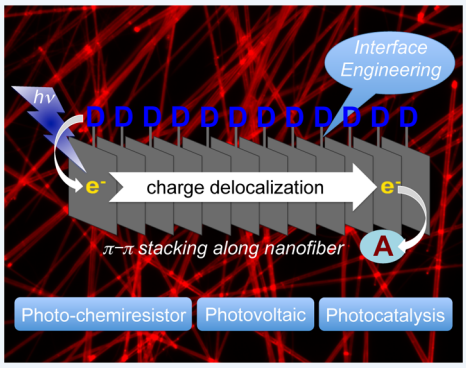

The photoconductivity generated with the nanofibril material is proportional to the charge carriers density, which in turn is determined by the kinetics balance of the three competitive charge transfer processes: (1) the photoinduced electron transfer from D to A (also referred to as exciton dissociation), generating majority charge carrier located in the nanofiber; (2) the back electron transfer; and (3) the charge delocalization along the nanofiber mediated by the $\pi-\pi$ stacking interaction. The relative rates of these charge transfer processes can be tuned by the molecular structure and nanoscale interface engineering. As a result, maximal photoconductivity can be achieved for different D–A nanofibril composites. The photoconductive nanomaterials thus obtained demonstrate unique features and functions when employed in photochemiresistor sensors, photovoltaics and photocatalysis, all taking advantages of the large, open interface of nanofibril structure. Upon deposition onto a substrate, the intertwined nanofibers form networks with porosity in nanometer scale. The porous structure enables three-dimensional diffusion of molecules (analytes in sensor or reactants in catalysis), facilitating the interfacial chemical interactions. For carbon nanotubes, the completely exposed π-conjugation facilitates the surface modification through $\pi-\pi$ stacking in conjunction with D–A interaction. Depending on the electronic energy levels of D and A parts, appropriate band alignment can be achieved, thus producing an electric field across the interface. Presence of such an electric field enhances the charge separation, which may lead to design of new type of photovoltaic system using carbon nanotube composite.

1. INTRODUCTION

One-dimensional (1D) nanomaterials, such as nanofibers and nanotubes, have been increasingly explored in various optoelectronic devices and systems to achieve both performance enhancement and size miniaturization, taking advantages of the 1D confined electronic properties and the large, open interface of the nanomaterials. However, most of these nanostructures are fabricated from inorganic semiconductors or carbon allotropes. The organic counterparts have been much less studied, despite their superior features including structural tunability of electronic and optical properties, ease of solution processing, and chemical flexibility for interface modification.[1−5] This discrepancy is largely due to the intrinsically low electrical conductivity of organic materials.

Photoinduced electron transfer (PET) from electron donor (D) to acceptor (A) has been widely used to enhance the electrical conductivity of organic materials. The conductivity thus attained is usually referred as photoconductivity, and the PET approach is often called photodoping. In organic photovoltaics, bulk heterojunctions of D and A allow for efficient PET and generation of photocurrent. However, tight electronic communication between D and A often leads to formation of a charge-transfer complex, which is conducive to charge recombination. The lack of long-range charge transport pathway in these materials also facilitates the charge recombination. Thus, to achieve photoconductivity, the ma-

Received: March 31, 2015
Published: September 28, 2015

DOI: 10.1021/acs.accounts.5b00176
Acc. Chem. Res. 2015, 48, 2705−2714

Scheme 1. Enabling Photoconductivity of D−A Nanofiber Composites, n-Type Fiber (Acting as A) Modified with D or p-Type Fiber (Acting as D) Modified with A

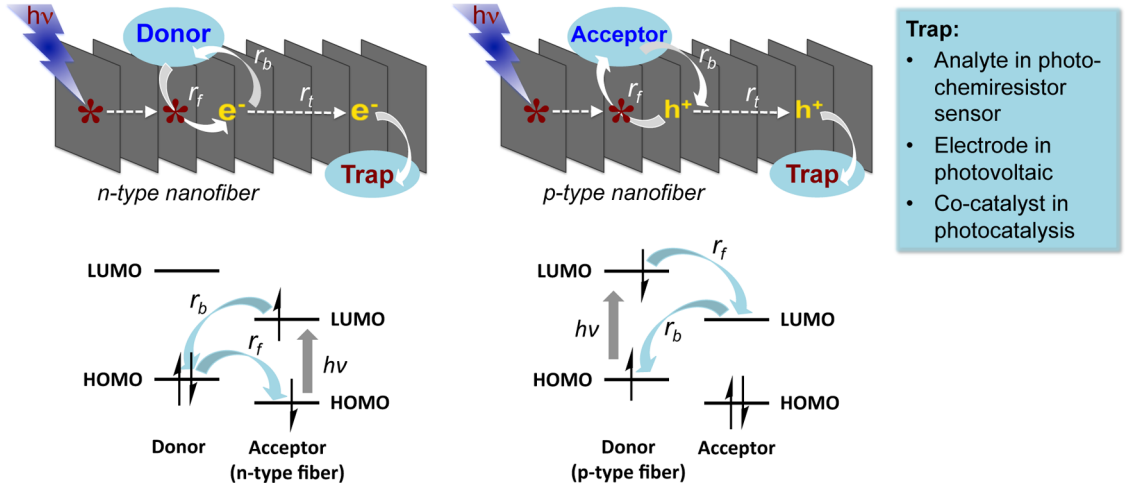

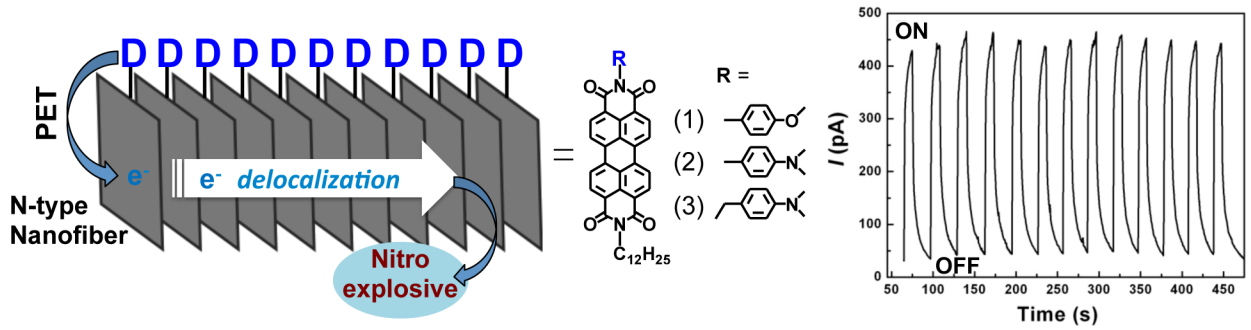

Figure 1. Tuning the PET within the building block molecules by changing the covalent linker of D and A. Two PTCDI molecules linked to *N*,*N*-dimethylaniline moiety (acting as D) are selected for studying the PET. As a control, the same PTCDI scaffold connected to methoxyphenyl moiety is used as a PET inactive building block. Shown on the right is the repeated photocurrent response measured over the fibers of molecule 3 under dark and white light irradiation (0.3 mW/mm^2). The photogenerated electron is delocalized along the nanofiber and can be captured by the surface adsorbed electron acceptor such as nitro-explosive compound. Reproduced from ref 17. Copyright 2010 American Chemical Society.

terial must be designed with both a tunable D−A interface that can be optimized to produce maximal charge separation, and an extended charge transport pathway to allow for further charge separation and eventual collection at electrodes. Organic nanofibers self-assembled from building block molecules can fulfill these two features by structural modification of the molecules at side groups and optimization of the intermolecular arrangement (π−π stacking), respectively.

In this Account, we will review our recent discoveries and breakthroughs on interface engineering and structural optimization of D−A nanofibril composites, which combined produce photoconductivity. Depending on the different structures and surface properties, these photoconductive nanofibers can be employed in sensors, photodetectors, photovoltaics, photocatalysis, and other optoelectronic systems. The tunable D−A interface, along with the structural flexibility of organic nanofibers, provides not only new designs for photoconductive materials, but also deep insight into the structure−property relationship that is critical for further improvement of performance and exploration of new functions. The nanofibril structures covered in this Account are mostly assembled from building-block molecules based on the derivatives of perylene tetracarboxylic diimide (PTCDI, see Figure 1 for an example), which forms an extremely robust class of materials with high thermal- and photostability, as practiced in many film devices and applications.[6,7] 1D self-assembly of PTCDIs has extensively been studied in our lab and others,[4,8] and various assembly methods have been developed to form well-defined nanofibers.

2. STRUCTURAL AND INTERFACIAL ENGINEERING OF D−A NANOFIBRIL COMPOSITES

2.1. Mechanism of Photoconductivity Generation

The nanofibers discussed in this Account are fabricated by self-assembly of molecules, for which the chemical protocols and methodologies were reviewed in our previous Account.[4] This bottom-up material fabrication allows for structural modification of the building block molecules in order to construct a D−A interface that will provide optimal charge separation (Scheme 1). Two types of D−A interface can be constructed: covalently linked D−A and noncovalent linking of D and A. The former is usually achieved by direct self-assembly of D−A molecules, while the latter is generally constructed using a postassembly method, for example, coating D (or A) onto the surface of n-type (or p-type) fibers preassembled. Photoinduced charge separation can be understood as exciton dissociation at the D−A interface. Due to the low dielectric constant of organic materials, the photogenerated excited state exists as a tightly bound electron−hole pair (e^-−h^+), referred to as Frenkel exciton. When it reaches the D−A interface, the exciton

DOI: 10.1021/acs.accounts.5b00176
Acc. Chem. Res. 2015, 48, 2705−2714

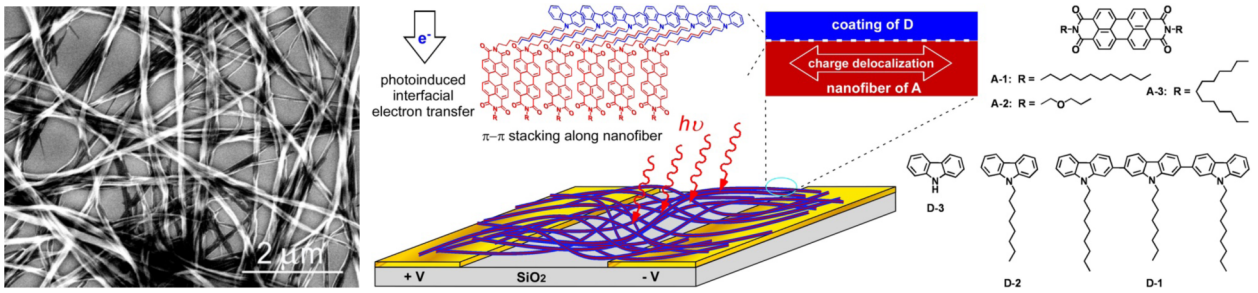

Figure 2. Nanofibril heterojunctions formed by coating of D molecules onto A nanofibers, for which the D–A interface is composed of the interdigitated alkyl chains of D and A. Shown at left is a SEM image of the nanofibers assembled from A-1. Reproduced from ref 18. Copyright 2010 American Chemical Society.

dissociates into free charges of e^- and h^+ driven by the energy level offset between D and A. To enhance the dissociation of exciton, the material must be designed to afford extended exciton diffusion. The nanofiber structure presented here is conducive to long-range exciton diffusion driven by the strong electronic coupling between the π–π stacks along the long axis of nanofiber.[9] Diffusion lengths exceeding 250 nm were recently attained for a PTCDI nanofiber at room temperature.[10] This length is much longer than those observed for conjugated polymers, usually in the range of a few nanometers.[7] The 1D enhanced exciton diffusion is consistent with the highly polarized emission observed for the same nanofiber; the latter is also directed along the π–π stacking.[11] Long range exciton diffusion enables the amplified fluorescence quenching of nanofibers by the surface adsorbed analytes;[4,12,13] that is, a single quencher on surface can quench the excited state of any component molecules within the exciton diffusion range.

The photoconductivity (σ) generated with the nanofibril material is determined by the density and mobility of the two charge carriers (electron and hole), as given in eq 1,

$$\sigma = e(n\mu_n + p\mu_p) \tag{1}$$

where e is the elementary charge, n and p are the density of electron and hole, and μ_n and μ_p are the mobility of electron and hole, respectively. For n-type materials, the major charge carrier is electron, and thus the conductivity will be mostly determined by the electron component, while the reverse case is for p-type materials. The density of the charge carriers photogenerated in the nanofiber is determined by the three competitive processes as illustrated in Scheme 1: (1) the photoinduced (forward) electron transfer (with rate r_f) between the D and A moieties, generating majority carrier located in the nanofiber; (2) the back electron transfer (rate r_b); and (3) the charge transport or delocalization (rate r_t) along the long axis of nanofiber. The former two depend on the D–A interfacial structure, including the distance and coupling geometry, while the latter is mostly determined by the π–π stacking arrangement between the building-block molecules within nanofiber.[14,15] Approximately, the density of the photogenerated charge carriers is proportional to the rate difference between the forward and back electron transfer ($r_f - r_b$), and the competitiveness of the charge transport along nanofiber against the back electron transfer, expressed as a ratio of $r_t/(r_t + r_b)$. Such relationship can be roughly described as eq 2.

$$n(or\ p) = C(r_f - r_b)\frac{r_t}{(r_t + r_b)} \tag{2}$$

where C is a constant intrinsic to the nanofiber.

Clearly, to attain maximal n or p (and thus the maximal photoconductivity, σ in eq 1), the values of r_f, r_b, and r_t must be balanced. On one hand, the faster the forward electron transfer (which can be tuned by the D–A distance), the larger the value of $(r_f - r_b)$ will be. On the other hand, a faster forward electron transfer is often accompanied by a faster back electron transfer, meaning r_b will become larger as well, leading to a decrease in the ratio $r_t/(r_t + r_b)$. This trade-off demands appropriate molecular design and structural engineering of the D–A system so as to produce maximal density of charge carriers.

2.2. Nanofibers of Covalent D–A Molecules

One way to approach photoconductivity is to assemble the building-block molecules containing covalently linked D–A units into nanofiber structures, for which efficient charge separation can be initiated by PET. However, it remains challenging to assemble D–A molecules into continuous 1D stacking, since the charge transfer interaction between the D and A parts often causes them stack on each other.[16] The bulk-mixed phase of D/A thus produced is conducive to loss of charge carriers through rapid charge recombination between D^+ and A^-. To solve this problem, amphiphilic D–A molecules based on the scaffold of PTCDI (Figure 1) were designed and synthesized, and fabricated into well-defined nanofibers (in the shape of a ribbon with thickness of only 5 nm) through self-assembly in solution.[17] The 1D molecular assembly is primarily driven by the π–π stacking between the perylene planes, together with the hydrophobic interaction between the alkyl side chains. The columnar π–π stacking of perylene scaffolds provides a conduit for efficient charge transport (here the electrons). Due to the similar molecular size and geometry, the three building-block molecules shown in Figure 1 produced approximately the same intermolecular arrangement, which allows for comparative investigation of the D–A structural dependence of the photoinduced charge separation.

Significant photoconductivity response was observed for the nanoribbons fabricated from molecule 3 when irradiated by white light irradiation, producing a photoswitching on/off ratio of ca. 10^3 under a applied electric field of 3.3 V/μm (Figure 1). The photoconversion efficiency was estimated as 63% under argon at 5 V/μm electric field; this efficiency is significantly higher than the values reported on the other nanofiber materials.[17] The photoconduction switching was also found to be fast and repeatable when turning the light irradiation on and off consequently as shown in Figure 1. The repeated photoresponse indicates high photostability of the PTCDI materials under ambient conditions. This is in contrast to many other organic semiconductor materials, which often suffer from

DOI: 10.1021/acs.accounts.5b00176
Acc. Chem. Res. 2015, 48, 2705–2714

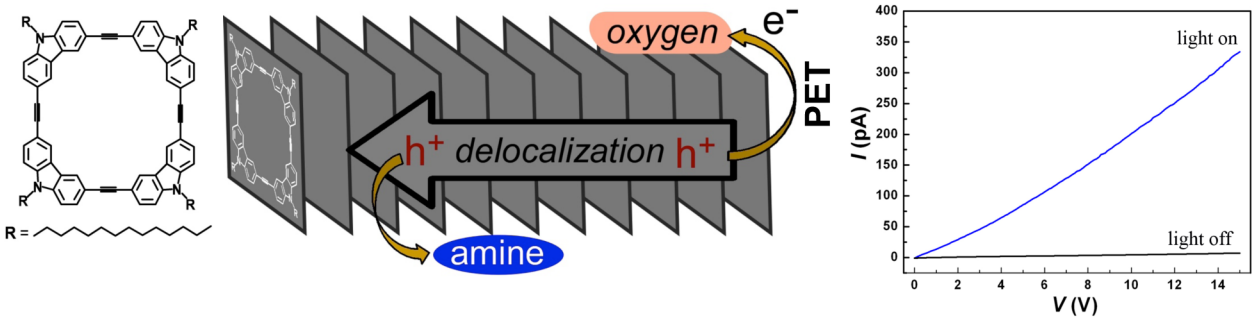

Figure 3. Photoconductivity enhancement of a p-type nanofiber fabricated from building block TDTC: PET from TDTC to oxygen (acting as A) generates holes as charge carrier flowing in the nanofiber. The hole will be quenched when encountering an electron donator (e.g., amine) adsorbed on the surface. Shown on right are the *I*−*V* curves measured on the TDTC nanofibers with and without white light irradiation (0.3 mW/mm^2). Adapted with permission from ref 19. Copyright 2010 The Royal Society of Chemistry.

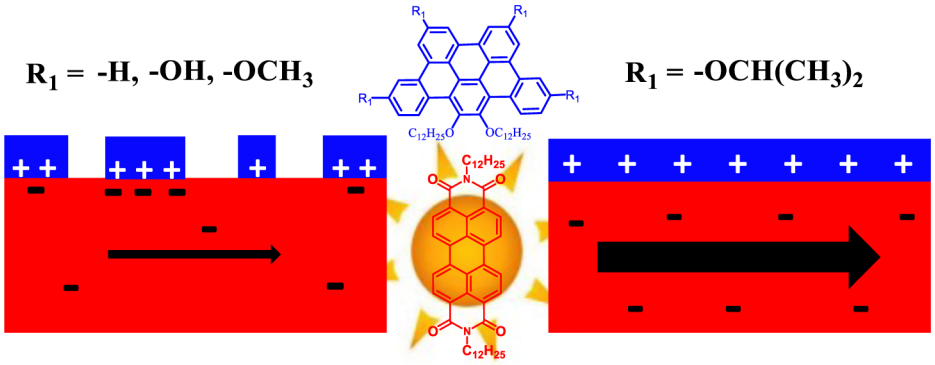

Figure 4. Schematic illustration of D−A nanofibril heterojunction composed of a PTCDI fiber coated with four different D molecules, D1−D4, which possess the same π-conjugate core, but are substituted with different peripheral side groups that determine the coating morphology, and thus affect the photoinduced charge separation with the PTCDI fiber. All four D molecules possess two dodecyl side chains at the same sites, which interdigitate with the dodecyl side chains of PTCDIs, forming the D−A interface. Reproduced from ref 20. Copyright 2013 American Chemical Society.

photobleaching. Remarkably, the nanoribbons fabricated from molecule 2 demonstrated almost no photoconductivity response (on/off ratio of only ca. 3) under the same experimental conditions. Considering the same D and A parts of these two molecules, the observed difference in photoconductivity response is apparently due to the different length of D−A linker (though only a slight difference of one more carbon in molecule 3). Although the direct D−A connection in molecule 2 results in faster forward electron transfer (r_f) compared to molecule 3, the back electron transfer (r_b) is also faster, thus becoming more competitive with the π−π electron delocalization (r_t) along the fiber. As a result, the ratio $r_t/(r_t + r_b)$ included in eq 2 becomes smaller (assuming that r_t, mostly determined by the π−π stacking of PTCDIs, remains about same). For this specific molecular system, controlling the back electron transfer is critical for maximizing the charge carrier density. Slowing the back electron transfer by increasing the D−A distance helps survive the charge separation state, thus allowing for further transport of electrons along the fiber.

2.3. Nanofibers with Noncovalent D−A Interface

The tunable D−A interface can also be obtained with PTCDI nanofibers using noncovalent molecular engineering, which usually offers more flexibility for structural optimization. Shown in Figure 2 is one such example based on a nanofibril heterojunction, for which the noncovalent D−A interface can be formed simply by coating D molecules onto the PTCDI nanofibers (ideally just one-step drop casting).[18] The D−A interface is primarily composed of the interdigitated alkyl side chains of D and A molecules, enabling efficient charge separation through PET process. The relatively wide D−A spacing thus formed (though not necessarily to be the same as the chain length due to nonregidity of alkyl chains) also helps prevent the charge recombination by slowing the back electron transfer as discussed above for covalent D−A system. The nanofiber structure not only creates large D−A interface for enhanced charge separation, but also provides continuous charge transport pathway for the photogenerated electrons, facilitating the charge collection at electrodes. Combination of these unique features makes the nanofibril heterojunction an ideal candidate for tuning and maximizing the photocondutivity.

By testing a series of D molecules that are modified with different side chains in combination with the different side chains of A part as shown in Figure 2, photoconductivity with on/off ratio of 10^4 was obtained.[18] The quantum yield of the photocurrent generation was measured to be ca. 8% at an electrical field of 2 V/μm under ambient condition. The photocurrent response was also found to be fast (on a time scale of ca. 200 ms) and reversible upon turning the light irradiation on and off. This prompt photoresponse, in combination with the high on/off ratio, implies great potential for the nanofibril heterojunctions to be employed in optoelectronics.

The noncovalent D−A interfacial engineering can also be applied to p-type nanofibril material, which acts as an electron

DOI: 10.1021/acs.accounts.5b00176
Acc. Chem. Res. 2015, 48, 2705−2714

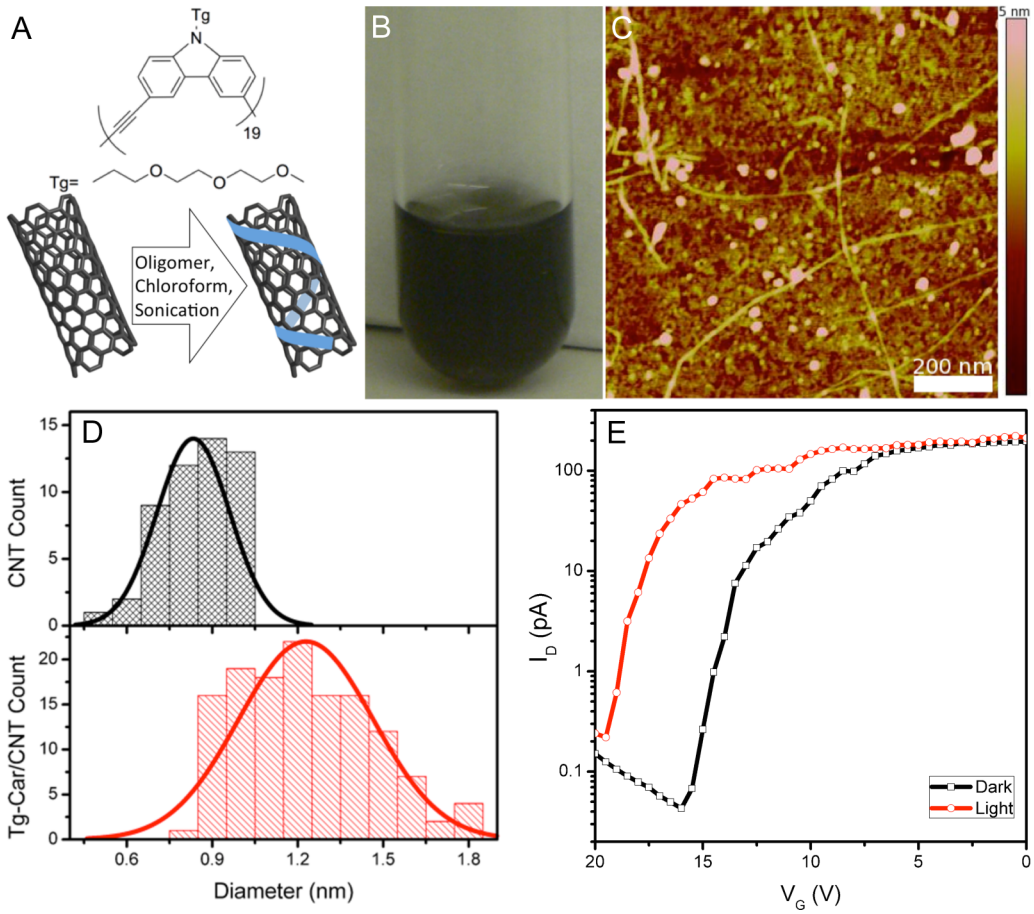

Figure 5. (A) Molecular structure of the Tg-Car oligomer and schematic illustration of the surface stacking onto single-wall CNT. (B) Photograph of the chloroform dispersion of Tg-Car/CNT (stable for over 3 years). (C) AFM image of Tg-Car/CNT deposited on a silicon substrate. (D) Histogram of CNT diameters measured by AFM before and after coating with Tg-Car. The coating of Tg-Car on the CNT surface is evidenced by a 50% increase in diameter. (E) Transfer characteristics of the FET devices fabricated with Tg-Car/CNT. Illumination with visible light results in an increase in current and a shift in threshold voltage. Adapted with permission from ref 21. Copyright 2014 John Wiley and Sons.

donor. Figure 3 shows such an example, where the p-type nanofibers were assembled from a carbazole-cornered, arylene-ethynylene tetracyclic macromolecule (named TDTC).[19] Due to the electron donating character of TDTC, the D−A interface can be simply formed between the nanofiber and the surface adsorbed oxygen molecule under ambient condition. Photo-excitation of the nanofiber initiates PET from TDTC to oxygen, producing holes flowing in the nanofiber as major charge carrier. In this case, intrinsic surface adsorption of oxygen provides an easy approach to building D−A interface. The nanofibers shown in Figure 3 exhibited large photo-conductivity response when irradiated with white light in air. The photoresponse was confirmed to be highly reversible by turning on and off the light irradiation. The repeatable testing proved the high photostability (against photobleaching) of the nanofiber materials.

2.4. Morphology Effect of Surface Coated D

With the success of noncovalent D−A interface engineering of the PTCDI nanofibers as shown in Figure 2, we have further explored the effects of molecular aggregation of D molecules on the photoconductivity of D−A nanofibril heterojunctions.[20] One-step drop casting often results in formation of molecular aggregate, especially when the D molecules are in relatively large conjugate structure. As shown in Figure 4, four D molecules (centered on tribenzopentaphene) modified with varying side groups were synthesized, and used for fabricating the D−A nanofibril composites. Due to the different side groups (determining the steric hindrance in balance with the $\pi-\pi$ stacking interaction), the four D molecules tends to assemble differently, leading to formation of molecular aggregates in different morphologies. While the bulky side groups of D4 molecule enforce homogeneous molecular distribution on the nanofiber surface, the small side groups of molecules D1−D3 are conducive to strong $\pi-\pi$ stacking aggregation, in favor of forming segregated particles around the nanofiber. As a result, the PTCDI nanofibers coated with D4 molecule demonstrated the highest photocurrent, with values much higher than those measured over the fibers coated with molecules D1−D3 under the same experimental conditions. Such morphology effect was even more pronounced after treating the nanofibril composites with solvent annealing, which thermodynamically improves the homogeneous molecular distribution of D4 molecules, and enhances molecular aggregation of D1−D3. Consequently, the photocurrent response of the nanofibers coated with D4 was further increased, whereas those coated with D1−D3 showed significant decrease in photocurrent. The decreased photo-current observed for the coating of D1−D3 is likely due to the strong local electrical field (i.e., high charge density) built up around the aggregate−nanofiber interface (as illustrated in Figure 4), which facilitates the charge recombination

DOI: 10.1021/acs.accounts.5b00176
Acc. Chem. Res. 2015, 48, 2705−2714

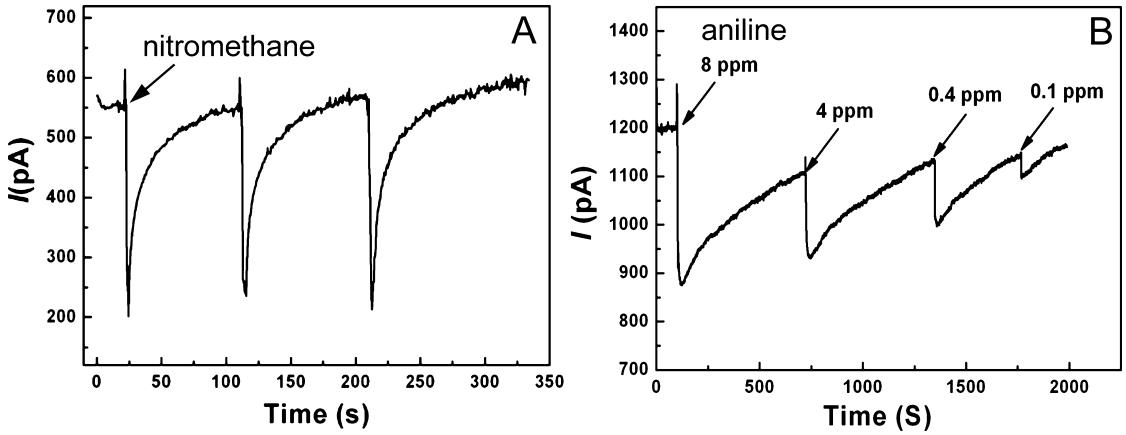

Figure 6. (A) Photocurrent change of the PTCDI nanofiber (shown in Figure 1) in response to the saturated vapor of nitromethane, tested consequently for three times. (B) Photocurrent change of the TDTC nanofiber (shown in Figure 3) when exposed to aniline vapor of various concentrations. (A) part adapted from ref 17. Copyright 2010 American Chemical Society. (B) part adapted with permission from ref 19. Copyright 2010 The Royal Society of Chemistry.

(increasing r_b in eq 2). These observations provide further insight into the structural understanding of the photoconductivity of D−A interfacial materials, particularly the dependence on the interface morphology, which in turn can be optimized through molecular design and supramolecular processing.

2.5. Noncovalent D−A Modification of Single-wall Carbon Nanotubes

The noncovalent D−A interface engineering developed for organic nanofibers can be extended to other fibril nanomaterials such as carbon nanotubes (CNTs),[21] which are now commercially available in high purity at a much lower cost than before. CNTs are unique in their completely exposed π-conjugation surface, which is conducive for surface modification through $\pi-\pi$ stacking in conjunction with D/A interaction. The materials shown in Figure 5 represent a unique case of noncovalent D−A modification of CNT, where a dual-functional oligomer (namely, Tg-Car) was employed to not only disperse the CNTs, but moreover forms a tunable D−A interface that enables efficient photoinduced charge separation.[21] The effective dispersion is due to the surface binding of oligomers that help solubilize CNTs in hydrophobic solvent with their long alkyl side chains. Effective dispersion of CNTs was also obtained in our lab using a different oligomer based on phenylene ethynylene unit.[22]

The photoinduced charge separation of Tg-Car/CNT composite was studied by fabricating the material into a field-effect transistor (FET) device. Under white light illumination the photocurrent was increased by over 3 orders of magnitude at positive gate voltage, and moreover the threshold voltage was shifted by 4.2 V compared to the value in darkness. In contrast, the pristine CNTs did not demonstrate such threshold shift. A more positive threshold voltage means an increase in hole concentration within the CNT (a typical p-type doping), which in turn indicates that the Tg-car oligomer acts as an electron acceptor, mainly caused by the band alignment at the oligomer/CNT interface. Such band alignment also forms an electric field across the interface at a voltage of 2.5 V. Existence of such electric field helps prevent the back electron transfer from the oligomer to CNT (decreasing r_b in eq 2), thus enhancing the charge separation. The surface photodoping presented herein may provide design criteria for D−A interface to enhance charge separation, leading to improved photovoltaic system using CNT composites.

3. APPLICATIONS OF D−A PHOTOCONDUCTIVE NANOFIBERS

3.1. Photochemiresistor Sensing for Chemical Vapor Detection

The D−A nanofibers shown in Scheme 1 can be developed into photochemiresistor sensors, which measure the change in photocurrent in response to the surface adsorption of analytes, which form trap sites. When deposited on a substrate, for example, a glass patterned with pairs of electrodes, the intertwined nanofibers form a porous "supernet" structure with a large surface area, which is conducive to vapor sensing by capturing target molecules from the air through molecular diffusion and surface adsorption. Upon capturing target molecules on surface, the nanofiber will either withdraw electron from the molecule or donate electron to it resulting in an increase or decrease in observed electrical conductivity.

The photoconductivity obtained for the n-type nanofibril materials shown in Figure 1 enables sensitive vapor detection of oxidative (electron withdrawing) species through chemiresistor sensor mode. When adsorbed on surface, these species deplete the electrons (here the major charge carrier), resulting in a decrease in observed photocurrent. To prove the sensing concept, the photoconductive nanofibers were tested toward the vapor of several nitro-based explosives, including 4-nitrotoluene, 4,6-dinitrotoluene, nitrobenzene, 1-chloro-4-nitrobenzene, and nitromethane, the vapor pressure of which ranges widely from tens of thousands ppm down to 0.1 ppm.[17] Figure 6A shows a typical photocurrent response when exposed to the saturated nitromethane vapor, for which the current was sharply decreased by as large as 65%. Such chemiresistor response was found to be highly reversible; that is, the photocurrent could be quickly recovered to the original value when the nitromethane vapor was removed. The quick sensor response is conducive to real-time, in-field detection.

Conversely, the p-type fiber fabricated from TDTC (Figure 3) demonstrated sensitive photocurrent response to the vapor of reductive agents such as amines, which deplete the holes from fiber. As shown in Figure 6B, the photocurrent measured on the nanofibers decreases dramatically when exposed to the

DOI: 10.1021/acs.accounts.5b00176
Acc. Chem. Res. 2015, 48, 2705−2714

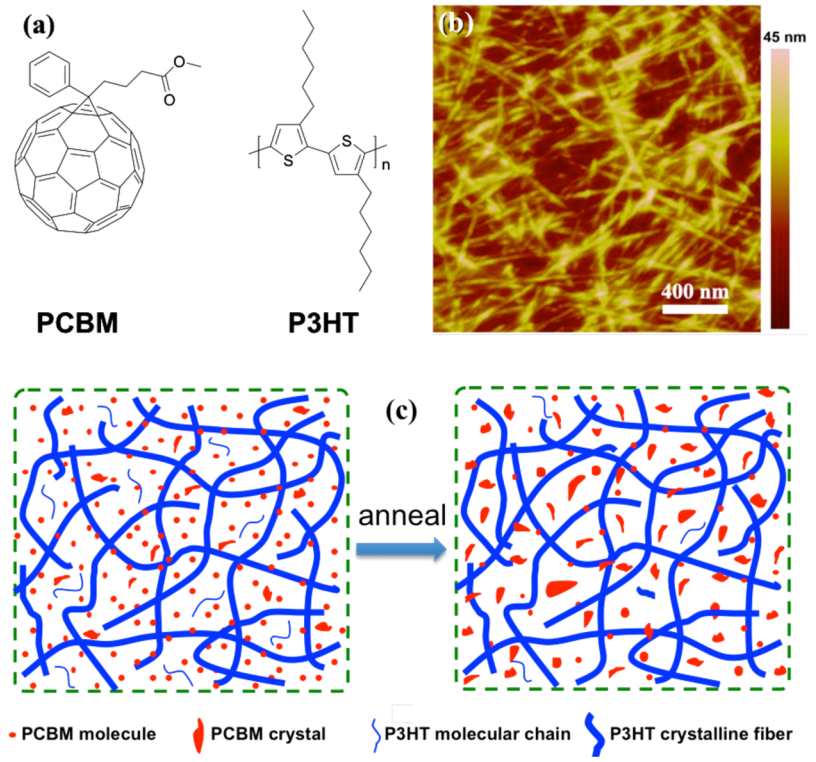

Figure 7. (a) Molecular structures of PCBM and regioregular P3HT used. (b) AFM image showing the fibril morphology of P3HT/PCBM film spun-cast from the aged solution in 1:1 (v/v) tetralin/xylene mixture solvent, where the nanofibers of P3HT were preformed. (c) Sketch showing the morphology change of the PCBM phase confined within the nanofibril network of P3HT under thermal annealing. Adapted with permission from ref 23. Copyright 2013 Elsevier.

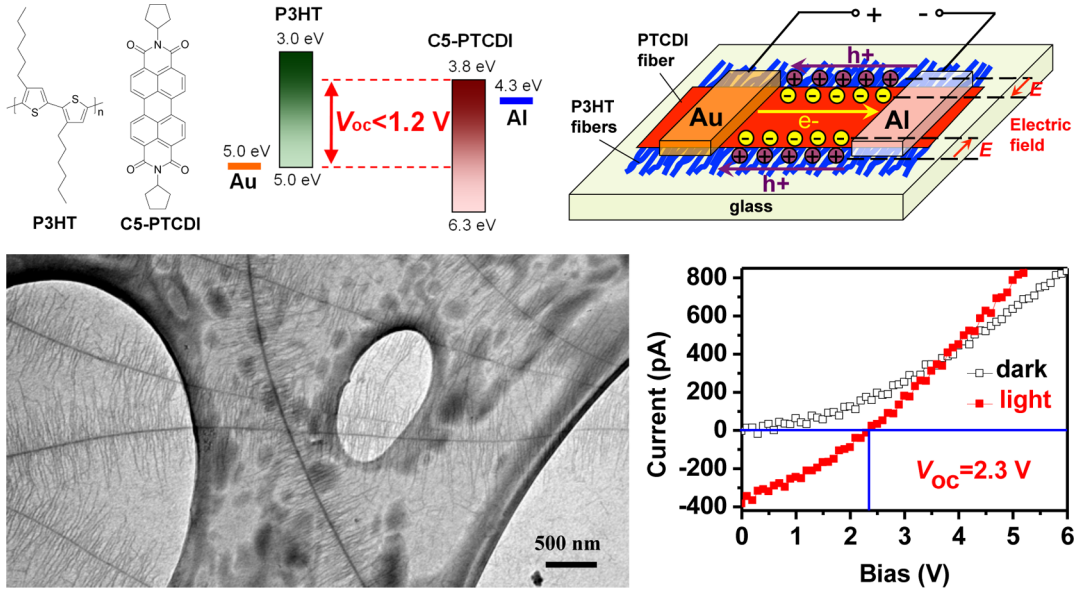

Figure 8. (Top panel) Molecular structures of C5-PTCDI and regioregular P3HT; the upper limit of photovoltage (V_{oc}) for the D−A junction of P3HT/C5-PTCDI caused by the energy level offset; shown on the right is a photovoltaic device fabricated with a single shish kebab of C5-PTCDI and P3HT. (Bottom panel) TEM image of the shish kebab fibril structure formed between the PTCDI and P3HT; *I*−*V* characteristics measured over the single shish kebab device under dark and light illumination (simulated AM1.5G). Adapted with permission from ref 24. Copyright 2014 The Royal Society of Chemistry.

aniline vapor.[19] Even under a low vapor concentration of 0.1 ppm, a significant sensor response (3% decrease in current) could still be observed. Based on the standard deviation of electrical measurement, the detection limit can be estimated to be as low as in sub-ppb range. Moreover, the sensor response observed was highly reversible, suited for application in continuous screening of chemicals.

3.2. D−A Nanofibril Heterojunction in Photovoltaics

The D−A nanofibril composites provide tunable bulk-heterojunction (BHJ) materials for organic solar cells to

DOI: 10.1021/acs.accounts.5b00176
Acc. Chem. Res. 2015, 48, 2705−2714

optimize the performance as evidenced from our recent research (Figure 7),[23] where the p-type nanofiber was fabricated from P3HT (the most common polymer used in BHJ solar cells) and the A part used was PCBM, the surface modified C60 that demonstrated the highest photoconversion efficiency when blended with P3HT. First, the large D−A interface enables efficient charge separation under illumination, while the long fibril phase facilitates the charge carrier transport. Second, the network formed by P3HT nanofibers can spatially retrain the diffusion of PCBM molecules, thereby inhibiting the formation of larger PCBM crystals when subject to thermal annealing. Large PCBM crystals are detrimental to photoinduced charge separation. As a result, a solar cell spun-cast from the P3HT/PCBM fibril composite can reach an efficiency of 3.4% even under ambient condition. Thermal annealing of the cell did not lead to increase in efficiency, implying a simple, one-step fabrication of BHJ solar cells. Even after high temperature annealing at 150 °C for 160 min, the device maintained about 80% of the initial efficiency, consistent with the strong thermal stability enabled by the nanofibril network of P3HT. In contrast, the film spun-cast from the homogeneous solution in chloroform demonstrated no fibril structure, and the photoconversion efficiency was only 0.5% due to the lack of charge transport pathway. Thermal annealing led to quick increase in efficiency up to 3.2%, though further annealing (after 15 min at 150 °C) caused degradation of the device, with efficiency decreasing back to the initial level of 0.5%. The decrease in efficiency is largely due to the formation of large crystals of PCBM.

The D−A nanofibril structure can also be fabricated between two types of nanofibers joined together, for example, in the form of a shish kebab as shown in Figure 8,[24] where the shish is a prefabricated PTCDI nanobelt, and kebabs are ultrafine nanofibers of P3HT (20 nm in diameter) growing perpendicularly from the side of PTCDI nanobelt via self-assembly in xylene solvent. The large D−A interface enables efficient photoinduced charge separation, and the electrons thus produced can flow along the shish, leaving the holes delocalized along the P3HT nanofibers. Due to the unbalanced charge transport in the PTCDI and P3HT phases, a high density of charge carriers are accumulated across the D−A interface, and the electric field thus established dominates the intrinsic photovoltage (V_{oc}). Indeed, when fabricated into a horizontal solar cell device, the shish kebab fibril composite demonstrated an anomalously high photovoltage, >2.0 V, which is much higher than the theoretical value (1.2 V) determined by the energy level offset between the HOMO of P3HT and LUMO of PTCDI. The unique shish-kebab D−A interface may help develop new materials and structures to further improve the photovoltaic performance of organic semiconductors.

3.3. D−A Nanofiber as Photocatalyst

The photoconductive D−A nanofibers, particularly those based on PTCDIs, can be employed as a photocatalyst to produce hydrogen from water following the mechanism illustrated in Scheme 1. The extended delocalization of electrons along the nanofiber enhances surface trapping by the cocatalyst deposited on the nanofiber, and the trapped electrons will reduce the surface protons to hydrogen. The LUMO level of PTCDIs is energetically suited for water reduction, with a driving force larger than 0.5 eV. Photocatalysis benefits from the large surface area of nanofibers, which allows for maximal interaction with the reactants. Photocatalysis was first examined with a PTCDI nanofiber directly coated with 0.5 wt % Pt nanoparticles as cocatalyst, which generated hydrogen under visible light illumination (>420 nm, 400 W xenon lamp), though the rate was slow, ca. 1.5 μmol g^{-1} h^{-1}.[25] The low reaction yield was likely due to the poor surface deposition of Pt nanoparticles, which in turn weakens the interfacial electron capture. To overcome this problem, we assembled the PTCDIs in mixture with graphitic carbon nitride (g-C_3N_4), which is among the most promising metal-free photocatalysts for H_2 production,[26] and proven effective for surface deposition of Pt particles. As expected, the PTCDI/g-C_3N_4 D−A composite demonstrated much increased rate of hydrogen generation, up to ca. 11 μmol g^{-1} h^{-1}.[27] This rate is also much higher than that obtained for the g-C_3N_4 photocatalyst without modification by PTCDI tested under the same conditions. Although exploration of the photocatalysis mechanism of PTCDI composite (regarding interfacial charge transfer and separation) is still underway, this initial observation indicates the great potential of using the D−A nanofibril materials for photocatalysis.

4. CONCLUDING REMARKS

In this Account, we summarized our recent research progress in construction, structural modification, and nanoscale engineering of D−A interfacial materials composed of organic nanofibers or other fibril structures like carbon nanotubes. The photoconductivity of these materials can be enhanced or optimized through various molecular designs and supramolecular processing, which in turn control the relative rates between photoinduced electron transfer, charge recombinatio,n and charge transport along the fiber. Depending on the property and morphology, the photoconductive materials thus fabricated can be used in chemiresistor sensors, photovoltaics, and photocatalysis, all taking advantages of the highly efficient charge separation within the D−A system.

In addition to the molecules covered in this Account, many other building block molecules (e.g., carbazole oligomers,[28] tribenzopentaphene,[29] expanded boardlike structure with dibenzo[fg,op]naphthacene cores,[30] triphenylene-containing π-conjugated macrocycles[31]) have also been synthesized and fabricated into well-defined nanofibers. Based on the solution self-assembly methodologies we developed before,[4] some new (advanced) processing methods have recently been developed to accommodate the assembly of different molecules; these methods include surface assisted self-assembly,[32] pH triggered hydrogelation,[33] and temperature-controlled reversible assembly of amphiphilic molecules.[34] Some of these nanofibers have already demonstrated unique optical or electronic properties as implied by the conductivity modulation,[31] chemiresistor sensing,[33] or amplified fluorescence quenching (sensing).[28] These observations indicate that the diverse molecular designs of π-conjugation system, in conjunction with the structural flexibility of D−A interface, will lead to further improvement of the efficiency of photoinduced charge separation, while still maintaining the nanofiber morphology suited for sensor and catalysis applications. Specific effort can be put onto the side group modification in order to tune the $\pi-\pi$ stacking configuration, and thus optimize the intermolecular charge delocalization rate (r_t in eq 2). A larger r_t will be more competitive to the back electron transfer process (r_b), thus leading to an increase in charge carrier density

DOI: 10.1021/acs.accounts.5b00176
Acc. Chem. Res. 2015, 48, 2705−2714

AUTHOR INFORMATION

Corresponding Author

*E-mail: LZANG@eng.utah.edu.

Notes

The author declares no competing financial interest.

Biography

Ling Zang is a USTAR professor at University of Utah, affiliated with Department of Materials Science and Engineering, Department of Chemistry, and Nano Institute of Utah. He received his B.S. in chemistry from Tsinghua University and Ph.D. in chemistry from the Chinese Academy of Sciences. His current research focuses on nanoscale imaging and molecular probing, organic semiconductors and nanostructures, optoelectronic sensors, and nanodevices, which may lead to real applications in the areas of security, renewable energy and clean environment. He was previously an Alexander von Humboldt Fellow, NSF CAREER Award winner, and K. C. Wong Foundation Research Fellow.

ACKNOWLEDGMENTS

The author thanks all the group members who contributed significantly to the work discussed in this Account. The work was supported by NSF (CHE 0641353, CHE 0931466, and CBET 730667), the Department of Homeland Security, Science and Technology Directorate under Grant Number (2009-ST-108-LR0005), ACS-PRF (45732-G10), NASA (NNX12AM67H), NSF IGERT (DGE0903715), and USTAR Program. The author is also grateful to Ben Bunes for his proofreading and discussion of the manuscript.

REFERENCES

(1) Zhao, Y. S.; Fu, H.; Peng, A.; Ma, Y.; Xiao, D.; Yao, J. Low-dimensional nanomaterials based on small organic molecules: preparation and optoelectronic properties. *Adv. Mater.* **2008**, *20*, 2859−2876.

(2) Kim, F. S.; Ren, G.; Jenekhe, S. A. One-Dimensional Nanostructures of π-Conjugated Molecular Systems: Assembly, Properties, and Applications from Photovoltaics, Sensors, and Nanophotonics to Nanoelectronics. *Chem. Mater.* **2011**, *23*, 682−732.

(3) Palmer, L. C.; Stupp, S. I. Molecular Self-Assembly into One-Dimensional Nanostructures. *Acc. Chem. Res.* **2008**, *41*, 1674−1684.

(4) Zang, L.; Che, Y.; Moore, J. S. One-Dimensional Self-Assembly of Planar-Conjugated Molecules: Adaptable Building Blocks for Organic Nanodevices. *Acc. Chem. Res.* **2008**, *41*, 1596−1608.

(5) Hoeben, F. J. M.; Jonkheijm, P.; Meijer, E. W.; Schenning, A. P. H. J. About Supramolecular Assemblies of pi-Conjugated Systems. *Chem. Rev.* **2005**, *105*, 1491−1546.

(6) Law, K.-Y. Organic Photoconductive Materials: Recent Trends and Developments. *Chem. Rev.* **1993**, *93*, 449−486.

(7) Hains, A. W.; Liang, Z.; Woodhouse, M. A.; Gregg, B. A. Molecular Semiconductors in Organic Photovoltaic Cells. *Chem. Rev.* **2010**, *110*, 6689−6735.

(8) Wurthner, F. Perylene bisimide dyes as versatile building blocks for functional supramolecular architectures. *Chem. Commun.* **2004**, 1564−1579.

(9) Hughes, R. E.; Hart, S. P.; Smith, D. A.; Movaghar, B.; Bushby, R. J.; Boden, N. Exciton dynamics in a one-dimensional self-assembling lyotropic discotic liquid crystal. *J. Phys. Chem. B* **2002**, *106*, 6638−6645.

(10) Chaudhuri, D.; Li, D. B.; Che, Y.; Shafran, E.; Gerton, J. M.; Zang, L.; Lupton, J. M. Enhancing Long-Range Exciton Guiding in Molecular Nanowires by H-Aggregation Lifetime Engineering. *Nano Lett.* **2011**, *11*, 488−492.

(11) Che, Y.; Yang, X.; Balakrishnan, K.; Zuo, J.; Zang, L. Highly Polarized and Self-Waveguided Emission from Single-Crystalline Organic Nanobelts. *Chem. Mater.* **2009**, *21*, 2930−2934.

(12) Che, Y.; Gross, D.; Huang, H.; Yang, D.; Yang, X.; Discekici, E.; Xue, Z.; Zhao, H.; Moore, J. S.; Zang, L. Diffusion-Controlled Detection of TNT: Interior Nanoporous Structure and Low HOMO Level of Building Blocks Enhance Selectivity and Sensitivity. *J. Am. Chem. Soc.* **2012**, *134*, 4978−4982.

(13) Che, Y.; Zang, L. Enhanced Fluorescence Sensing of Amine Vapor Based on Ultrathin Nanofibers. *Chem. Commun.* **2009**, 5106−5108.

(14) Che, Y.; Datar, A.; Yang, X.; Naddo, T.; Zhao, J.; Zang, L. Enhancing One-dimensional Charge Transport through Cofacial pi-Electronic Delocalization: Conductivity Improvement for Organic Nanobelts. *J. Am. Chem. Soc.* **2007**, *129*, 6354−6355.

(15) Delgado, M. C. R.; Kim, E.-G.; da Silva Filho, D. A.; Bredas, J. L. Tuning the Charge-Transport Parameters of Perylene Diimide Single Crystals via End and/or Core Functionalization: A Density Functional Theory Investigation. *J. Am. Chem. Soc.* **2010**, *132*, 3375−3387.

(16) Pisula, W.; Kastler, M.; Wasserfallen, D.; Robertson, J. W. F.; Nolde, F.; Kohl, C.; Mullen, K. Pronounced Supramolecular Order in Discotic Donor-Acceptor Mixtures. *Angew. Chem., Int. Ed.* **2006**, *45*, 819−823.

(17) Che, Y.; Yang, X.; Liu, G.; Yu, C.; Ji, H.; Zuo, J.; Zhao, J.; Zang, L. Ultrathin N-type Organic Nanobelts with High Photoconductivity and Application in Optoelectronic Vapor Sensing of Explosives. *J. Am. Chem. Soc.* **2010**, *132*, 5743−5750.

(18) Che, Y.; Huang, H.; Xu, M.; Zhang, C.; Bunes, B. R.; Yang, X.; Zang, L. Interfacial Engineering of Organic Nanofibril Heterojunctions into Highly Photoconductive Materials. *J. Am. Chem. Soc.* **2011**, *133*, 1087−1091.

(19) Che, Y.; Yang, X.; Zhang, Z.; Zuo, J.; Moore, J. S.; Zang, L. Ambient photodoping of p-type organic nanofibers: highly efficient photoswitching and electrical vapor sensing of amines. *Chem. Commun.* **2010**, *46*, 4127−4129.

(20) Huang, H.; Chou, C.-E.; Che, Y.; Li, L.; Wang, C.; Yang, X.; Peng, Z.; Zang, L. Morphology control of nanofibril donor-acceptor heterojunction to achieve high photoconductivity: exploration of new molecular design rule. *J. Am. Chem. Soc.* **2013**, *135*, 16490−16496.

(21) Bunes, B. R.; Xu, M.; Zhang, Y.; Gross, D. E.; Saha, A.; Jacobs, D. L.; Yang, X.; Moore, J. S.; Zang, L. Photodoping and Enhanced Visible Light Absorption in Single-Walled Carbon Nanotubes Functionalized with a Wide Band Gap Oligomer. *Adv. Mater.* **2015**, *27*, 162−167.

(22) Zhang, Z.; Che, Y.; Smaldone, R. A.; Bunes, B. R.; Moore, J. S.; Zang, L. Reversible Dispersion and Release of Carbon Nanotubes Using Foldable Oligomers. *J. Am. Chem. Soc.* **2010**, *132*, 14113−14117.

(23) Li, L.; Jacobs, D. L.; Che, Y.; Huang, H.; Bunes, B. R.; Yang, X.; Zang, L. Poly(3-hexylthiophene) nanofiber networks for enhancing the morphology stability of polymer solar cells. *Org. Electron.* **2013**, *14*, 1383−1390.

(24) Li, L.; Jacobs, D. L.; Bunes, B. R.; Huang, H.; Yang, X.; Zang, L. Anomalous high photovoltages observed in shish kebab-like organic p−n junction nanostructures. *Polym. Chem.* **2014**, *5*, 309−313.

(25) Chen, S.; Jacobs, D. L.; Xu, J.; Li, Y.; Wang, C.; Zang, L. 1D Nanofiber Composites of Perylene Diimides for Visible-light-driven Hydrogen Evolution from Water. *RSC Adv.* **2014**, *4*, 48486−48491.

(26) Wang, Y.; Wang, X.; Antonietti, M. Polymeric Graphitic Carbon Nitride as a Heterogeneous Organocatalyst: From Photochemistry to Multipurpose Catalysis to Sustainable Chemistry. *Angew. Chem., Int. Ed.* **2012**, *51*, 68−89.

(27) Chen, S.; Wang, C.; Bunes, B. R.; Li, Y.; Wang, C.; Zang, L. Enhancement of Visible-light-driven Photocatalytic H2 Evolution from Water over g-C3N4 through Combination with Perylene Diimide Aggregates. *Appl. Catal., A* **2015**, *498*, 63−68.

(28) Zhang, C.; Che, Y.; Yang, X.; Bunes, B. R.; Zang, L. Organic nanofibrils based on linear carbazole trimer for explosive sensing. *Chem. Commun.* **2010**, *46*, 5560−5562.

DOI: 10.1021/acs.accounts.5b00176
Acc. Chem. Res. 2015, 48, 2705−2714

(29) Chou, C.-E.; Li, Y.; Che, Y.; Zang, L.; Peng, Z. Synthesis, self-assembly and photovoltaic applications of tribenzopentaphene derivatives. *RSC Adv.* **2013**, *3*, 20666−20672.
(30) He, J.; Agra-Kooijman, D. M.; Singh, G.; Wang, C.; Dugger, C.; Zang, L.; Kumar, S.; Hartley, C. S. Board-like dibenzo[fg,op]-naphthacenes: Synthesis, characterization, self-assembly, and liquid crystallinity. *J. Mater. Chem. C* **2013**, *1*, 5833−5836.
(31) Dutta, T.; Che, Y.; Zhong, H.; Laity, J.; Dusevich, V.; Murowchick, J.; Zang, L.; Peng, Z. Synthesis and Self-Assembly of a Triphenylene-Containing Conjugated Macrocycle. *RSC Adv.* **2013**, *3*, 6008−6015.
(32) Datar, A.; Gross, D. E.; Balakrishnan, K.; Yang, X.; Moore, J. S.; Zang, L. Ultrafine nanofibers fabricated from an arylene ethynylene macrocyclic molecule using surface assisted self-assembly. *Chem. Commun.* **2012**, *48*, 8904−8906.
(33) Datar, A.; Balakrishnan, K.; Zang, L. One-dimensional Self-assembly of a Water Soluble Perylene Diimide Molecule by pH Triggered Hydrogelation. *Chem. Commun.* **2013**, *49*, 6894−6896.
(34) Li, L.; Che, Y.; Gross, D.; Huang, H.; Moore, J. S.; Zang, L. Temperature Controlled Reversible Nanofiber Assembly from an Amphiphilic Macrocycle. *ACS Macro Lett.* **2012**, *1*, 1335−1338.

DOI: 10.1021/acs.accounts.5b00176
Acc. Chem. Res. 2015, 48, 2705−2714